



Synthesis, Enantio-Separation and Molecular Docking Study of Hesperidin-Oxime



CrossMark

Meriem Bouanini^[a], Nasser Belboukhari^{[a]*}, Khaled Sekkoum^[a], Djawhara Haddad^[a]

^a Bioactive Molecules and Chiral Separation Laboratory, Faculty of exact sciences, Tahri Mohammed University, Istiklal street PO 417 Bechar, 08000, Algeria

Abstract

This study aims to synthesize hesperidin oxime from hesperidin, chiral separation by HPLC method and comparative study of two enantiomers as anti-inflammatory agents by docking them with Proto-oncogene serine/threonine-protein kinase Pim-1 using MOE software (4.2). The structure of the synthesized product was validated through UV, IR, ¹H-NMR, and ¹³C-NMR spectroscopic techniques. Hesperidin-oxime was separated chirally in normal phase mode employing polysaccharide-based chiral stationary phases, namely Chiralcel® OD-H, Chiralcel® OD-RH, and CHIRALPAK® AD-3R, under both normal and polar organic phase modes. Molecular docking shows that S-hesperidin oxime gave better binding affinity towards pim-1 compared to R-hesperidin oxime.

Keywords: Hesperidin oxime, HPLC, molecular docking, Pim-1, anti-inflammatory

1. Introduction

Plants contain high levels of flavonoids, which are polyphenolic compounds that protect plants from parasites and illnesses [1-3]. Flavonoids are structurally classified into a variety of compounds, the most prominent of which are flavones, flavonols, and flavanones. These compounds are well-documented for exhibiting a range of biological activities, such as antioxidant, antiviral, anti-inflammatory, and anticancer effects [4-6]. Hesperidin (figure 1), commonly known as Vitamin P [7-9], is a bioflavonoid [10-12] that belongs to the flavonoid class known as flavanones [13]. It is a cheap by-product found nearly exclusively in citrus fruits. Hesperidin (3',5,7-trihydroxy-4'-methoxyflavanone-7- α -L-rhamnopyranosyl (1 \rightarrow 6)- β -D-glucoside or -7-rutinoside) is a chiral flavanone glycoside, containing two parts. An aglycone part is hesperetin (C₁₆H₁₄O₆), which chemically is a 5,7-dihydroxy-2-(3'-hydroxy-4'-methoxyphenyl) chroman-4-one, and a sugar part is rutinoside.

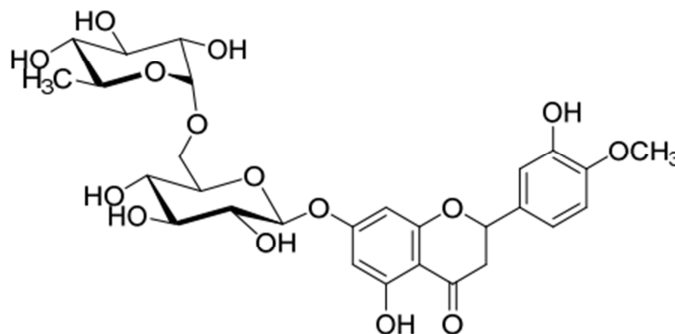


Figure 1: Structure of Hesperidin.

Displayed in Figure 1 is the conjugate formed between hesperetin and rhamnosyl- α -1,6-glucose. Hesperidin is considered to be one of the most abundant citrus flavonoids isolated from the discarded peel of an ordinary orange. Hesperidin, along with Diosmin, a flavone glycoside, is used to treat venous insufficiency [14-16]. The concentration of hesperidin in orange juice

*Corresponding author e-mail: belboukhari.nasser@univ-bechar.dz; (Nasser Belboukhari).

Received date 04 November 2024; Revised date 09 January 2025; Accepted date 22 January 2025

DOI: 10.21608/ejchem.2025.333625.10739

©2025 National Information and Documentation Center (NIDOC)

ranges from 200 to 600 mg/L [16-17]. As a result, pulp-containing orange juice contains more of this flavonoid than pulp-free juice. Hesperidin's effects on illness prevention and therapy have received much attention recently [18]. It functions in various biological roles, including antioxidant, antibacterial, antiulcer, anti-inflammatory, anti-carcinogenic, and vascular protective activities.

Hesperidin has been employed in treating patients with vascular abnormalities, particularly those involving vessel fragility and enhanced permeability linked to bruising [19]. In vitro studies have shown that Hesperidin exhibits antifungal activity versus *Aspergillus fumigatus*, *Trichoderma glaucum* and *Botrytis cinerea* at doses ranging from 1 to 10 µg. However, it was discovered to be inert against *Aspergillus niger*. At a dose of 0.25 mM, Hesperidin did not entirely inhibit the development of *Penicillium expansum*, *Aspergillus flavus*, *Fusarium semitectum* and *Aspergillus parasiticus*, as well as higher concentrations in subsequent studies. In vitro tests showed that hesperidin had no inhibitory impact on *Candida albicans* or *Saccharomyces cerevisiae* [19-21].

Oximes (R1R2C@NOH) constitute a class of hydroxylamines in which R1 represents an organic side chain, while R2 can be either hydrogen (yielding an aldoxime) or an aromatic group (yielding a ketoxime). In organic synthesis, oximes and their derivatives serve as essential intermediates. Beyond their utility as a protective group, the oxime functional group readily connects with significant chemical groups, including carbonyl, amino, nitro, and cyano functionalities [22].

Serving as vital intermediates, oximes are integral to the production of agrochemical and pharmaceutical compounds, and they have been used in a variety of important medicinal and synthetic chemistry applications [12]. Many organic drugs used to treat organophosphate (OP) poisoning include oxide-type functional groups. Acute OP toxicity inhibits acetylcholinesterase (AChE), although oximes are expected to be somewhat effective in treating OP poisoning because they reactivate AChE [23,24].

The current study focuses on the chiral separation of hesperidin oxime by HPLC, Optimizing analytical conditions with the aid of polysaccharide-based chiral stationary phases. The compounds were produced in a single reaction step involving hesperidin and hydroxylamine, and comparative study of two enantiomers as anti-inflammatory agents by docking them with Proto-oncogene serine/threonine-protein kinase Pim-1 using MOE software (4.2).

2. Materials and methods

2.1. Reagents and solvents

Hesperidin was purchased from Sigma-Aldrich (Schnell Dorf, Germany), and hydroxylamine hydrochlorides along with sodium acetate trihydrate were acquired from Fluka Buches.

2.2. Synthesis of hesperidin oxime

Hesperidin oxime was synthesized by combining 0.01 mol (6.1 g) of hesperidin with 0.01 mol (0.69 g) of hydroxylamine hydrochloride in 20 mL of methanol and 0.01 mol (1.35 g) of sodium acetate trihydrate in water. The reaction mixture was subjected to reflux in a water bath for 48 hours with constant stirring. Following cooling to ambient temperature and the addition of 10 mL of dichloromethane, a white precipitate appeared, which was filtered and washed with water. The resulting yield of the product was 63%, with a melting point of 204 °C.

2.3. IR

The AGILENT Cary 630 FTIR spectrophotometer, fitted with a diamond ATR accessory, was employed to record IR spectra for both solid and liquid materials, thus removing the necessity for sample preparation. Wave numbers are indicated in cm⁻¹.

2.4. NMR

Nuclear magnetic resonance (NMR) spectroscopy was carried out using a BRUKER spectrometer, with measurements taken at 400 MHz for ¹H NMR and 100 MHz for ¹³C NMR. Chemical shifts are denoted in ppm, and coupling constants are shown in Hertz.

2.5. Chromatographic separation

The analysis was performed using a Shimadzu LC-2030 series system, which included an automatic injector for a sample loop of 1-100 µL, a double pump system with vacuum degassing, and a Shimadzu UV detector with adjustable wavelengths. Data from chromatographic analyses were acquired, recorded, and processed using LC Lab Solution software (Shimadzu, Tokyo, Japan). A 10 µL injection volume was used, with the UV wavelength configured based on each compound's λ_{max}. Separations were carried out in isocratic mode at 25°C, with flow rates adjusted as required.

2.6. Chiral Stationary Phases (CSPs)

This research investigated four analytical stationary phases. The Exsil C-18 ODS achiral stationary phase (250 × 4.6 mm ID, 5 µm particle size) was utilized alongside three other polysaccharide-based chiral stationary phases (CSPs) from Chiral

Technologies Europe (Illkirch, France): Chiralcel® OD-H, Chiralcel® OD-RH, and CHIRALPAK® AD-3R. HPLC-grade solvents employed in the study included methanol (MeOH), water (H₂O), and hexane (HEX). Analytes were prepared in methanol with concentrations between 0.5 and 1 mg mL⁻¹. The injection volume was set to 20 µL, and the UV detector wavelength was fixed at 285 nm. Chromatographic separations took place in isocratic mode at a flow rate of 0.5 mL min⁻¹, which could be modified for particular requirements at ambient temperature.

2.7. Molecular docking study

In this study, we utilized molecular docking to investigate potential interactions between hesperidin-oxime and Proto-oncogene serine/threonine-protein kinase Pim-1.

2.7.1 Preparation of ligand

Version 21.0 of the chemDraw program was used to sketch the 2D structures of hesperidin oxime, and chem3D was used to transform them to 3D. hesperidin-oxime preparations are optimized geometrically, with their initial positions, orientations, and torsions identified. Utilizing the MOE software (4.2), farther more, by adding hydrogen atoms to the structure, lowering the energy, and storing the result in the (Moe*) format.

2.7.2 Preparation of the protein

The online Protein Data Bank database (www.rcsb.org) offered access to the previously solved 3D crystal structure of pim-1, which has a resolution of 2.85Å. Utilizing the alpha-numeric PDB ID 2O65 <https://www.rcsb.org/structure/2O65>. The receptor is produced by eliminating all linked ligands and crystallographic water molecules. The atoms' type and connectivity were then verified using automated correction to avoid interference during molecule docking. The active site of Pim-1 is identified using its crystalline structure, and the required residues are selected for docking studies and saved as PDB format.

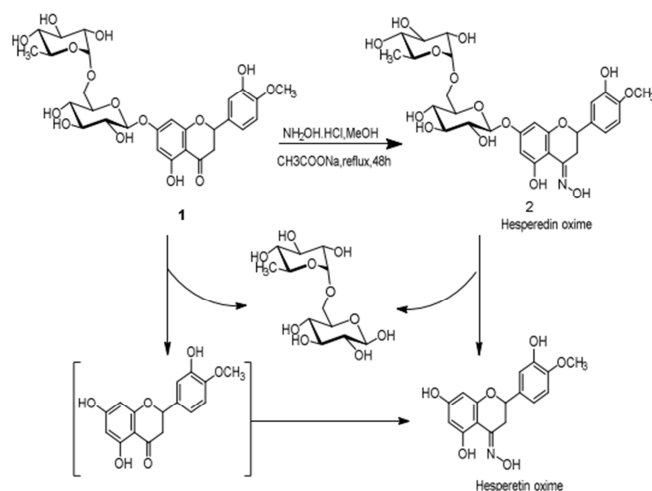
2.7.3 Molecular Docking

In the docking process, the ligand is inserted into the active site of the receptor, and the optimal orientation and conformation that yields the highest binding affinity are then sought after. Based on critical interactions with important active site residues and the highest affinity scores, the most likely binding conformations were selected. The combination of geometric and empirical scoring functions has been employed to achieve this [25,26].

3. Results and discussion

3.1. Synthesis of hesperidin oxime

The hesperidin oxime derivative (compound 2) was synthesized directly from hesperidin by treating it with hydroxyl amine in refluxing methanol. And as shown in Scheme 1, the isolated products were formed through a series of two reactions: the formation of the oxime and the cleavage of the heteroside bond by nucleophilic attack of the primary amine onto the anomeric carbon of rutinoside, resulting in the release of a phenoxide anion, a good leaving group. No intermediates were isolated; hence, the precise order of these two stages could not be determined. Scheme 1 showcases the reaction yield, which ranged from 63%. Spectral data processing was employed to validate the structures of the synthesized products, incorporating UV, IR (the spectra of all products did not display any absorption associated with (C=O)), and 1H and 13C NMR, which indicated an absence of rutinoside. The hesperitin oxime was synthesized by Naik and Harini [27].



Scheme 1: One-pot synthesis of hesperidin-oxime 2 from hesperidin 1

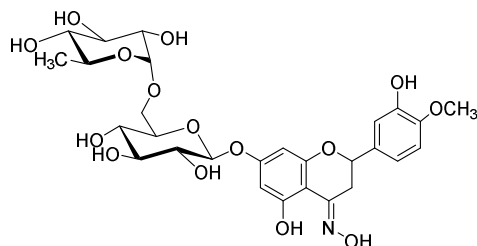


Figure 2: Structure of hesperidin-oxime 2

3.2. Characterization data for compounds

3.2.1 Hesperidin

3',5,7-trihydroxy-4'-méthoxyflavone-7- α -L-rhamnopyranosyl (1 \rightarrow 6)- β -D-glucoside: beige powder, mp 250–253 °C, UV_{max} (MeOH): 286 (band I); 330 (band II), IR (KBr, cm⁻¹)

¹H NMR 400 MHz, DMSO-d₆, δ ppm) 12.06 (s, 1H, 5-OH), 9.05 (s, 1H, 3'-OH), 6.95-6.92 (m, 3H, H-2', H5' & H-6'), 6.11 (d, J = 2.4 Hz, 1H, H-6), 6.10 (d, J = 2.0 Hz, 1H, H-8), 5.56 (dd, J = 12.3 Hz & 3.2 Hz, 1H, H-2), 5.44 (d, J = 4.7 Hz, 1H, H-1^{Glu}), 5.20-5.16 (m, 2H, H-1^{Rhm}, 6^{Glu}-OH), 5.02 (m, 1H, 4^{Rhm}-OH), 3.81 (m, 1H, H-3 ax), 3.77 (dd, J = 3.2 Hz, 1H, H-3 eq), 3.63 (s, 3H, 4'-OCH₃), 1.09 (d, J = 6.4 Hz, 3H, H-6^{Rhm}).

¹³C NMR (100MHz, DMSO, δ ppm) 198.9 (C-4), 164.7 (C-7), 163.5 (C-5), 162.9 (C-9), 146.9 (C-4'), 144.6 (C-5'), 131.4 (C-1'), 115.9 (C-2'), 114.6 (C-6'), 100.8 (C-10), 97.9 (C-6), 95.3 (C-8), 78.1 (C-2), 55.2 (4'-OCH₃), 42.1 (C-3), 17.8 (C-6Rhm).

3.2.2 Hesperidin oxime

(2-(3'-hydroxy-4'-méthoxyphényl)-5-hydroxy-4-(hydroxyylimino)-7-O-rutinosé)-chromane 2: brown powder, yield 63 %, mp 200–204 °C, UV_{max} (MeOH): 285 (band I); 325 (band II), IR (KBr, cm⁻¹): 3415 (OH, strong), 2967 (CH₃), 3389 (C=N-OH), 1503 (C=C), 1181 (C-O).

¹H NMR 400 MHz, DMSO-d₆, δ ppm) 12.23 (s, 1H, 5-OH), 11.25 (s, N-OH), 8.25 (s, 1H, 3'-OH), 6.89-6.90 (m, 3H, H-2', H5' & H-6'), 6.33 (d, J = 2.4 Hz, 1H, H-6), 6.05 (d, J = 2.0 Hz, 1H, H-8), 5.42 (dd, J = 12.3 Hz & 3.2 Hz, 1H, H-2), 5.38 (d, J = 4.7 Hz, 1H, H-1^{Glu}), 5.25-5.17 (m, 2H, H-1^{Rhm}, 6^{Glu}-OH), 5.11 (m, 1H, 4^{Rhm}-OH), 3.90 (m, 1H, H-3 ax), 3.87 (dd, J = 3.2 Hz, 1H, H-3 eq), 3.71 (s, 3H, 4'-OCH₃), 1.07 (d, J = 6.4 Hz, 3H, H-6^{Rhm}).

¹³C NMR (100MHz, DMSO, δ ppm) 166.9 (C-4), 165.1 (C-7), 163.0 (C-5), 162.6 (C-9), 147.8 (C-4'), 145.3 (C-5'), 130.3 (C-1'), 116.7 (C-2'), 114.1 (C-6'), 102.3 (C-10), 98.7 (C-6), 96.8 (C-8), 77.8 (C-2), 53.4 (4'-OCH₃), 41.5 (C-3), 17.6 (C-6Rhm).

3.3 Enantioseparation of hesperidin oxime

To isolate the chiral substances and identify all potential enantiomers, three chiral stationary phases were utilized: Normal-coated, normal-immobilized, and reversed-coated phases were utilized. An achiral conventional C-18 bonded stationary phase (Figure 3) was applied to assess the clarity of the products, yielding a distinct peak that confirmed the purity of the investigated compounds.

To achieve optimal separation of the hesperidin oxime enantiomers, the chromatographic conditions were refined for polar organic phase and normal phase modes using Chiralcel® OD-H [cellulose tris(3,5-dimethyl phenyl carbamate) coated on 5 μ m silica gel], reversed-phase CHIRALCEL® OD-RH [cellulose tris(3,5-dimethyl phenyl carbamate) coated on 5 μ m silica gel], and Chiralpak® AD-3R [amylose tris(3,5-dimethyl phenyl carbamate) immobilized on 3 μ m silica gel], with the structure depicted in Figure 5. Hesperidin enantioseparation using HPLC on polysaccharide CSPs has already been reported in several studies [28-32]. However, its oxime derivatives demand further exploration.

Table 1: Chromatographic data for the separation of hesperidin oxime by Chiral HPLC

Chiral stationary phases	Product	Mobile phase	Flow rate (ml/min)	T1 (Min)	T2 (Min)	'k1	'k2	α	Rs
Chiralcel®OD-H	2	EtOH-HEX (50-50)	0,5	4,23	5,25	2,01	4,35	1,56	1,19
		MeOH-H2O (80-20)		1.54	3.54	2.09	6.09	1.66	2.90
		MeOH 100%		6.57	7.37	2.15	2.42	1.52	1.22

Chiralcel®OD-RH	2	MeOH-H ₂ O (80–20)	0,5	2,87	,16	1,86	4,11	2,22	5,19
		MeOH 100%		1,48	2,44	0,32	1,18	1,07	3,67
		EtOH- Hex (50–50)		1,66	2,86	1,09	3,09	1,03	1,19
Chiralpak® AD-3R	2	MeOH-H ₂ O (70–30)	0,5	2,52	3,11	2,14	2,55	1,16	1,14
		EtOH- Hex (50–50)		4,82	5,63	3,56	3,56	3,82	1,12
		MeOH 100%		2,12	,11	2,75	2,86	1,19	1,15

Chiral stationary phases derived from polysaccharides, Cellulose and amylose have demonstrated their efficacy in HPLC for the separation of chiral pharmaceuticals across normal, reversed, and polar organic phase modes. All columns demonstrated good resolution; Both chiral stationary phases (CSPs) demonstrated effective interactions with the solutes, resulting in appropriate retention factor values. Optimal resolution was obtained for compound 2, hesperidin oxime ($R_s = 5.19$) (Figure 5), at a flow rate of 0.5 mL/min with a mobile phase mixture of 80% MeOH and 20% H₂O on the Chiralcel® OD-RH. In contrast, the minimum resolution was observed with hesperidin oxime on Chiralpak® AD-3R ($R_s = 1.12$) at the same flow rate, utilizing a mobile phase of 50% EtOH and 50% HEX. When the columns are arranged in descending order by R_s , their enantioseparation ability decreases in the following sequence: Chiralcel®OD-RH > Chiralcel®OD-H > Chiralpak®IA. It is worth noticing cellulose derivatives have better chiral separation than amylose. The cellulose tris (3,5-dimethyl phenyl carbamate) coating on silica gel achieves superior enantioselectivity for hesperidin oxime and shorter retention times, which may be attributed to the polarity of the methanol-water system. Compound 2 did not separate well on Chiralpak®AD-3R.

Incorporating water into the mobile phase significantly impacts the chiral recognition mechanisms of polysaccharide-based CSPs for various reasons, primarily because of water's strong solvation impact on polymer-based chiral selectors. This shift in solvation alters how the CSPs interact with their enantiomers, thereby increasing the potential for effective resolution. Methanol is often utilized as the organic phase in reversed-phase chromatography because of its low viscosity and UV absorbance, with elution typically achieved using an aqueous/alcohol solution. The reversed-phase mode is characterized by reduced separation times and increased resolution values, which can be primarily attributed to polarity becoming a crucial factor during aqueous/alcohol elution, thereby amplifying the solvation effect. The mechanisms of chiral recognition for cellulose and amylose derivatives differ due to the unique higher-order structures of the cellulose and amylose CSPs, along with variations in the configurations of the glucose residues and their connections. The stiffness and linearity of the cellulose derivatives' organization, as opposed to the more helical shape of the amylose derivatives, explains why cellulose columns have better chiral separation capabilities than the latter. The helices of cellulose and amylose, They are characterized as left-handed 3-fold (3/2) and left-handed 4-fold (4/1) structures, with cellulose enantiomers possessing a chiral surface created by distinct grooves [33, 37].

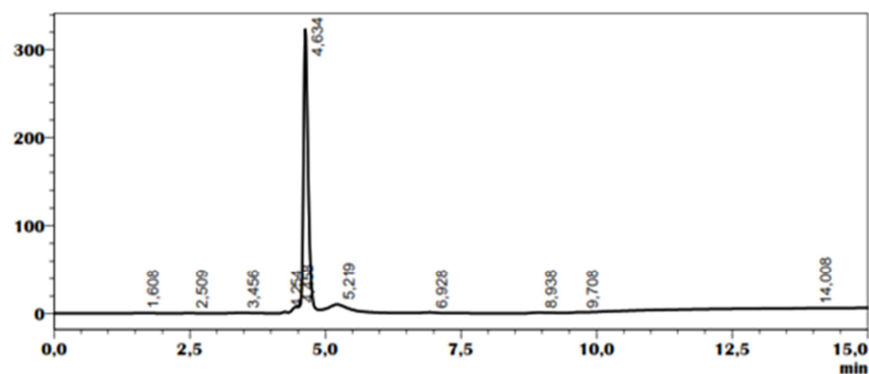


Figure 3: Chromatogram for determining the purity of hesperidin oxime; mobile phases CSP C-18 being MeOH

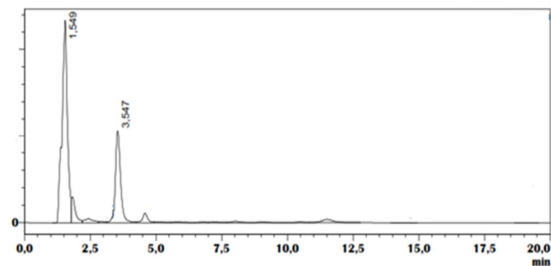


Figure 4: HPLC chromatograms of the enantiomeric separation of hesperidin oxime; CSP CHIRALCEL®OD-H; mobile phases MeOH-H₂O (80-20), flow rates 0.5 ml/min; temperature 25°C, UV detector set at 285 nm.

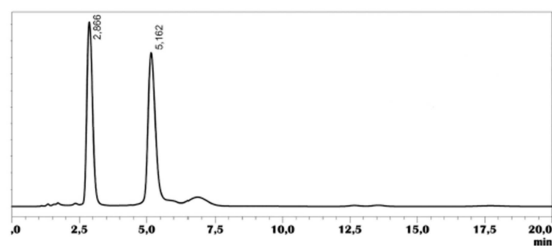


Figure 5: HPLC chromatograms of the enantiomeric separation of compounds 2; CSP CHIRALCEL®OD-RH; mobile phases MeOH-H₂O (80-20), flow rates 0.5 mL/min; temperature 25°C, UV detector set at 285 nm.

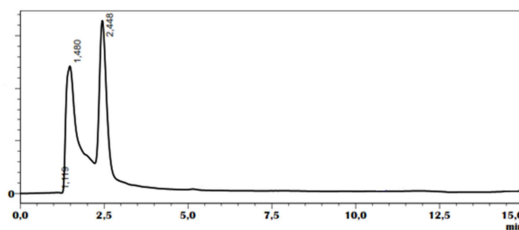


Figure 6: HPLC chromatograms of the enantiomeric separation of compounds 2; Chiralpak® OD-RH CSP; mobile phases MeOH 100%, flow rates 0.5 ml/min; temperature 25°C, UV detector set to 285 nm.

3.4 Molecular docking study

The binding affinity of hesperidin-oxime to the PIM-1 enzyme was examined through a molecular docking study. The results generated negative energy and a small RMSD of less than 2 Å, indicating a precise prediction[38-40]. Table 2 summarizes the study-specific binding energy (kcal/mol), RMSD values (Å) and type of interaction with PIM-1.

Table 2: The results of docking, the binding energy (kcal/mol), RMSD (Å) values and Interactions residues and type interaction with PIM-1

Compounds	BindingEnergy (Kcal /mol)	RMSD (Å)
S-hesperidin-oxime	-9.3	1.78
R-hesperidin-oxime	-7.9	1,93

The Table 2 shows that S- hesperidin-oxime has a low affinity binding value of -9.3 kcal / mol which is value is lower than R- hesperidin-oxime -7.9 kcal / mol. Accordingly, the S- hesperidin-oxime has a more stable bond to PIM-1 than R- hesperidin-oxime with RMSD value 1.78 and 1.93 (Å) respectively. This value is supported by the number of interactions formed between the ligands and PIM-1.

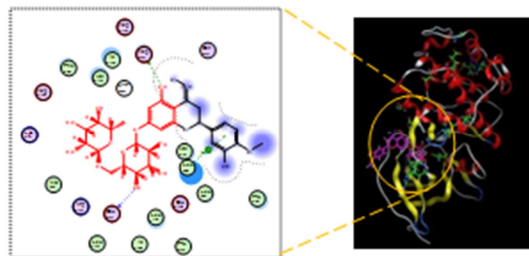


Figure 7: 3D and 2D docked pose depiction of S- hesperidin-oxime.

When investigating the interaction of S- hesperidin-oxime with the residues in the enzyme's active site, it was observed that it made six different vanderwalls interactions, two distinctive hydrophobic interactions and six different π interactions. Four different vanderwalls interactions were achieved with ASP_{A185}, GLU_{A124}, GLU_{A121} and GLU_{A89} residues, while the ASP_{A128} and ASP_{A131} residues formed vanderwalls interactions towards oxygen atom in the molecule. The hydrophobic interaction formed with ARG_{A122} and LYS_{A67} amino acid. Consequently, all π interaction formed are derived from the S- hesperidin-oxime molecule via amino acids VAL_{A126}, LEU₁₂₀, ILE_{A185}, LEU_{A174}, LEU_{A44} and VAL₅₂ (Figure 7).

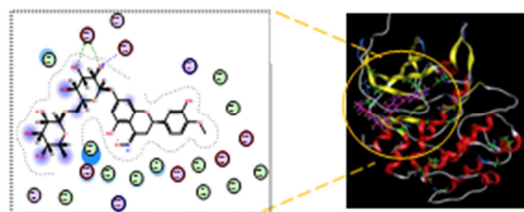


Figure 8: 3D and 2D docked pose depiction of R- hesperidin-oxime.

When the complex structure of the R- hesperidin-oxime compound with PIM-1 is examined, it is observed that vanderwalls interactions, hydrophobic interactions and π interactions come to the fore. The ASP_{A131} and ASP_{A121} residues formed vanderwalls interactions towards oxygen atom in the molecule, while three different vanderwalls interactions were achieved with GLU_{A124}, ASP_{A128}, ASP_{A186}, residues. The hydrophobic interactions were achieved with ARG_{A122} and LYS_{A67} residues. Five different π interactions were achieved with PHE_{A49}, LEU_{A174}, VAL_{A126}, ILE_{A185}, and VAL_{A52} residues, while the π interaction was constructed from the benzene ring to LEU_{A44} amino acid (Figure 8). According to figure 8 and 9, the R- hesperidin-oxime conformation has a greater number of interaction than R- hesperidin-oxime conformation.

4. Conclusions

The aim of this endeavour is to produce hesperidin oxime and analyze its enantioseparation through three Polysaccharide-based chiral stationary phases were utilized in both normal and polar organic phase modes, with Chiralcel® OD-RH providing the optimal separation outcomes for hesperidin oxime in reversed-phase mode. The study further examined the influence of chiral stationary phase properties on chiral separation. The results of the current research offer valuable insights into the molecular mechanisms underlying the anti-inflammatory activity of hesperidin oxime and pave the way for further exploration of its therapeutic potential.

5. References

1. Wang X, Cheng S. (2006). Solvent-free synthesis of flavanones over aminopropyl-functionalized SBA15. *J Catalysis Commun*; 7: 689-695.
2. Maltese F, Erkelens C. (2009). Identification of natural epimeric flavanone glycosides by NMR spectroscopy. *Food Chemistry*; 116:575-579.
3. Davies KM et Schwinn KE. (2006). Molecular Biology and Biotechnology of Flavonoid Biosynthesis. In: Andersen Ø Met Markham KR (éd) *Flavonoids: Chemistry, Biochemistry and Applications*. CRC Press, Boca Raton, US, pp.143-218.
4. Bouanani, M., Belboukhari, N., Menéndez, J.C., Sekkoum, K., Cheriti, A. Aboul-Enein, H.Y. (2018). Chiral separation of novel iminonaringenin derivatives; *Chirality*, 30: 484–490.
5. Zaid, M.E.A., Belboukhari, N., Sekkoum, K., Ramos, J.C.M., Aboul-Enein, H.Y. (2019). Analysis of different factors affecting a liquid chromatographic chiral separation of some imino-hesperetin compounds; *SN Applied Sciences*, 1: 1444.
6. Rahou, I., Sekkoum, K., Belboukhari, N., Cheriti, A., Aboul-Enein, H.Y. (2016). Liquid chromatographic separation of novel 4-amino-flavanes series diastereomers on a polysaccharide-type chiral stationary phase; *Journal of Chromatographic Science*, 54: 1787–1793.
7. Majumdar S et Srirangam R. (2009). Solubility, Stability, Physicochemical Characteristics and In Vitro Ocular Tissue Permeability of Hesperidin: A Natural Bioflavonoid. *Pharmaceutical Research*. 26:1217-1225.
8. Shen J, Nakamura H, Fujisaki Y, Tanida M, Horii Y et al. (2009). Effect of 4G- α -glucopyranosyl hesperidin on brown fat adipose tissue- and cutaneous-sympathetic nerve activity and peripheral body temperature. *Neuroscience Letters*. 461:30–35.

9. Kobayashi S, Tanabe S, Sugiyama M et Konishi Y (2008). Transepithelial transport of hesperetin and hesperidin in intestinal Caco-2 cell monolayers. *Biochimica et Biophysica Acta*. 1778:33–41.
10. Salas MP, Céliz G, Geronazzo H, Daz M et Resnik SL. (2011). Antifungal activity of natural and enzymatically-modified flavonoids isolated from citrus species. *Food Chemistry*. 124:1411–1415.
11. Garg A, Garg S, Zaneveld LJD et Singla AK. (2001). Chemistry and Pharmacology of The Citrus Bioflavonoid Hesperidin. *Phytotherapy Research*. 15:655–669.
12. Sun Y, Zhang H, Sun Y, Zhang Y, Liu H. (2010). Study of interaction between protein and main active components in Citrus aurantium L. by optical spectroscopy. *Journal of Luminescence*. 130:270–279.
13. Lin JK et Weng MS. (2006). Flavonoids as Nutraceuticals. In: Grotefeld E (éd) *The Science of Flavonoids*. Springer, US, pp. 213–238.
14. Hosseinimehr SJ, Ahmadi A, Beiki D, Habibi E et Mahmoudzadeh A. (2009). Protective effects of hesperidin against genotoxicity induced by ^{99m}Tc-MIBI in human cultured lymphocyte cells. *Nuclear Medicine and Biology* 36:863–867.
15. Rajasekaran A, Sivagnanam G et Xavier R. (2008). Nutraceuticals as therapeutic agents: A Review. *Research J. Pharm. and Tech.* 01(04):328–340.
16. Manach C, Morand C, Gil-Izquierdo A, Bouteloup-Demange C et Rémésy C. (2003). Bioavailability in humans of the flavanones hesperidin and narirutin after the ingestion of two doses of orange juice. *European Journal of Clinical Nutrition*. 57:235–242.
17. Erdman JW, Balentine D, Arab L, Beecher G, Dwyer JT et al (2007). Flavonoids and Heart Health: Proceedings of the ILSI North America Flavonoids Workshop, May 31–June 1, 2005, Washington, DC 1–4. *The Journal of Nutrition*. 137:718S–737S.
18. Kamaraj S, Anandakumar P, Jagan S et al. (2010). Modulatory effect of hesperidin on benzo(a)pyrene-induced experimental lung carcinogenesis with reference to COX-2, MMP-2 and MMP-9. *European Journal of Pharmacology*. 649 :320–327.
19. Lu Y, Zhang C, Bucheli P et Wei D. (2006). Citrus Flavonoids in Fruit and Traditional Chinese Medicinal Food Ingredients in China. *Plant Foods for Human Nutrition*. 61: 57–65.
20. Remya J, Manoj K, et al. (2023). Pharmaceutical characterisation and exploration of arkeshwara rasa in MDA-MB-231 cells. *Journal of ayurveda and integrative medicine*
21. Hazem K.A, Sarhan, Ahmed M.A Saleh et al (2021). The protective role of Diosmine, Hesperidin combination against heavy metals toxicity in wistar albino rats : Biochemical, Immunohistochemical and molecular studies. *Egyptian journal of chemistry*. 64 :4531–4543.
22. Ozyurek M, Akpınar D, Bener M, Turkan B, Guclu K, Apak R. (2014). Novel oxime based flavanone, naringin-oxime: Synthesis, characterization and screening for antioxidant activity. *J Chem-Biol Interact*; 212: 40–46.
23. F. Worek, P. Eyer, N. Aurbek, L. Szinicz, H. Thierman. (2007). Recent advances in evaluation of oxime efficacy in nerve agent poisoning by in vitro analysis. *Toxicol. Appl. Pharmacol.* 219 226–234.
24. G.O. Puntel, N.R. de Carvalho, P. Gubert, A.S. Palma, C.L.D. Corte, D.S. Avilaa, M.E. Pereira, V.S. Carratu, L. Bresolin, J.B.T. da Rocha, F.A.A. Soares. (2009). Butane-2,3- dionethiosemicarbazone: an oxime with antioxidant properties, *Chem-Biol. Interact.* 177 153–160.
25. Veedamali S. Subramanian, Samir Attoub, Tahir A. Rizvi, Thomas E. Adrian and Sandeep B. Subramanya. (2023). Molecular Docking Identifies 1,8-Cineole (Eucalyptol) as A Novel PPAR γ Agonist That Alleviates Colon Inflammation, *Int. J. Mol. Sci.*, 24, 6160. <https://doi.org/10.3390/ijms24076160>.
26. Ty Viet Pham, Hanh Nhu Thi Hoang, Hoai Thi Nguyen, Hien Minh Nguyen, Cong Thang Huynh, Thien Y Vu, Anh Thu Do, Nguyen Hoai Nguyen, and Bich Hang Do. (2021). Anti-Inflammatory and Antimicrobial Activities of Compounds Isolated from *Distichochlamys benenica*. *BioMed Research International*, <https://doi.org/10.1155/2021/6624347>.
27. N. Naik, S. Harini (2014). Synthesis of novel hesperetin oxime esters: a new discernment in their antioxidant potential. *International Journal of Pharmaceutical Sciences and Research*; Vol. 5(4): 1482–1489.
28. Aboul-Enein. (2001) HPLC High-performance liquid chromatographic enantioseparation of drugs containing multiple chiral centers on polysaccharide-type chiral stationary phases. *J Chromatogr A*; 906 : 185–193.
29. Belboukhari N, Cheriti A, Roussel C, Vanthuyn N. (2010). Chiral separation of hesperidin and naringin and its analysis in a butanol extract of *Launea arborescens*. *Nat Prod Res* ;247 : 669–681.
30. Rahou I, Belboukhari N, Sekkoum K, Cheriti A, Aboul-Enein H. Y. (2014). Chiral separation of 4-iminoflavan derivatives on several polysaccharide-based chiral stationary phases by HPLC. *Chromatographia*; 77: 1195–1201.
31. Roussel C, Bonnet B, Piedriere A. (2001). Suteu C. J Chirality Enantioselective correlation between retention factor and lipophilicity index in chiral separation on cellulose and amylose tris(3,5-dimethylphenylcarbamate) CSPs in reversed mode: A case study; 13: 56–61.
32. Caccamese S, Chilleemi R. (2009). Racemization at C-2 of naringin in pummelo (*Citrus grandis*) with increasing maturity determined by chiral high-performance liquid chromatography. *J. Chromatogr. A*; 1217: 1089–1093.
33. Lu WJ, Ferlito V, Xu C, Flockhart DA, Caccamese S. (2011). Enantiomers of naringenin as pleiotropic, stereoselective inhibitors of cytochrome P450 isoforms. *J Chirality*; 23:891–896.
34. Curti V, Di Lorenzo A, Rossi D, Martino E, Capelli E, Collina S, Daglia M. (2017). Enantioselective modulatory effects of naringenin enantiomers on the expression level of miR-17-3p involved in endogenous antioxidant defenses. *J Nutrients*; 9: 1–13.
35. Belboukhari N. (2012). Enantioseparation of hydroxyflavonones on amylose and cellulose CSPS by HPLC methods. *J Chromatogr Separation Techniq*; 3 : 67–68.
36. Lahmer N, Belboukhari N, Cheriti A. (2011). Méthodes et techniques de la séparation chirale des flavanones. *J Phytochem Bio Sub*; 5:1–4.
37. Rahou I, Sekkoum K, Belboukhari N, Cheriti A, Aboul-Enein HY. (2016). Liquid chromatographic separation of novel 4-amino-flavanes series diastereomers on a polysaccharide-type chiral stationary phase. *J Chromatogr Sci*; 54: 1787–1793.
38. Balaji Venkataraman, Saeeda Almarzoogi, Vishnu Raj, Bhoomendra A. Bhongade, Rajesh B. Patil, G. Widiyarti, Firdayani, M. Hanafi, S. Kosela, and E. Budianto. (2019). "Molecular Docking of Citronellol, Geraniol and Ester Derivatives as Pim 1 Kinase Inhibitor of Leukemia Cancer." *Jurnal Kimia Valensi*, vol. 5, no. 2, pp. 133–142, Nov., doi: 10.15408/jkv.v5i2.7195.
39. A. Belal et al. (2023). "Design of new captopril mimics as promising ACE inhibitors: ADME, pharmacophore, molecular docking and dynamics simulation with MM-PBSA and PCA calculations," *Journal of Taibah University for Science*, vol. 17, no. 1, , doi: 10.1080/16583655.2023.2210348.
40. N. Rahmadania Hasnaa and R. (2022). Trijuliamos Manalu, "Molecular Docking of Turmeric Active Compounds (*Curcuma longa* L.) against Main Protease in Covid-19 Disease," *East Asian Journal of Multidisciplinary Research (EAJMR)*, vol. 1, no. 3, pp. 353–364, [Online]. Available: <https://journal.formosapublisher.org/index.php/eajmr>.